increased cell viability by suppressing the activation of the ER stress pathway factors (16). Interestingly, exogenous Derlin-1 resulted in a decrease in the amount of mutant SOD1, and a lesser decrease in that of wild-type SOD1 in transfected cells. In addition, reduced SOD1 protein expression was observed in the microsomal fraction of wild-type and mutant SOD1 cells (16). Furthermore, Chromogranins, components of neurosecretory vesicles, interact with mutant forms of SOD1 that are linked to ALS, but not with wild-type SOD1 (17). These results suggest that Derlin-1 and Chromogranins may act as chaperone-like proteins to promote the secretion of SOD1 mutants. In ALS, the mutant SOD1-binding protein could play an important role through the ER stress pathway. There are a lot of ER-related chaperone proteins in neurons. In these proteins, Derlin-1 and Chromogranin bind to mutant SOD1. These two proteins may be the link to co-localization of mutant SOD1 and PDI.

PDI is an ER-specific chaperone and is linked to the accumulation of misfolded proteins in many neurodegenerative diseases (5). In this study, we have shown the localization of PDI in neuronal cells. PDI prevents the neurotoxicity associated with ER stress and protein misfolding, but NO blocks the enzyme's protective effect through the S-nitrosylation of PDI. This inhibition of PDI leads to ER stress, which can induce apoptosis (5). Recently, S-nitrosylation of PDI in patients with ALS was reported (8).

The levels of S-nitrosylated PDI were increased in transgenic mutant SOD1 mouse and human SALS spinal cord tissues. Hence, despite upregulation, PDI is also functionally inactivated in ALS (8). NO-induced S-nitrosylation of PDI inhibits its enzymatic activity, leading to the accumulation of polyubiquitinated proteins in ALS model mice (8). Furthermore, overexpression of PDI decreased mutant SOD1 aggregation, inclusion formation, ER stress induction, and toxicity, whereas small interfering RNA targeting PDI increased mutant SOD1 inclusion formation, indicating a protective role for PDI against SOD1 misfolding (8). Thus, PDI prevents the neurotoxicity associated with ER stress and misfolding in ALS. In addition, PDI was present in cerebrospinal fluid and was aggregated and widely distributed throughout the motor neurons of patients with SALS (18).

The accumulation of SOD1 is a link to the pathogenesis of FALS (3). Nevertheless, the accumulation of SOD1 is not observed in SALS. The mechanism of SALS may be different from FALS. TDP-43 is the major component of LBHIs and TDP-43 is seen in patients with SALS, but TDP-43 is not the only protein to contribute to the pathology of SALS. Further study is needed to elucidate the mechanism of progressive accumulation of TDP-43 in neurons.

Another pathological hallmark of ALS is swollen neurites. Axonal transport has two components: transport of vesicles and mitochondria by kinesin and related proteins (fast transport) and movement of the major structural components of the neuron, many enzymes, and other cytoplasmic proteins (slow transport). Slow transport can be divided into two components based on the rate of movement and containing the neurofilament proteins tubulin and actin, and containing tubulin, actin, and other cytoplasmic proteins (19). Retardation of slow axonal transport is a very early event in mice expressing the FALS-linked SOD1 (G37R) and SOD1 (G85R) mutations (19). In SOD1 (G85R) mutant mice, this is the earliest known abnormality, arising months before any pathological changes can be detected. Tubulin transport slows more dramatically at earlier stages, whereas the transport of neurofilaments and other cargo yet to be identified is affected at later time points, indicating a worsening of the defect, and presumably the underlying neuronal health and function, with time. This is consistent with the slow accumulation of damage over a long period, ultimately culminating in late onset of disease in both mice and humans. Further support for a disruption in slow axonal transport early in disease comes from the obvious proximal axon swellings in both SOD1 (G37R) and SOD1 (G85R) mice (19). The known neurofilament dependent slowing of axonal transport, combined with the accumulation

of neurofilaments in ALS, suggests that an important aspect of toxicity may arise from damage to transport (19).

In this study, we have revealed anti-PDI-antibody-immunopositive NCIs in the patients with SALS and FALS. Furthermore, PDI was co-localized with TDP-43 and SOD1 in NCIs. We assume that NO inhibited PDI and led to the accumulation of unfolded proteins in ALS. Abnormal TDP-43 and SOD1 or other proteins may be accumulated in NCIs and cause ER stress in ALS. In degenerated motor neurons, ER and other organelles are probably destroyed and injured. As PDI is working in neurons as a chaperone it may bind to TDP-43 or SOD1, and become included in NCIs. But the PDI in the NCIs may be a non-functional protein. We propose the mechanism of action of PDI recruitment to NCIs to be as follows. First, many unfolded proteins can accumulate in both cytosol and ER lumen of the motor neurons of patients with ALS, and these unfolded proteins can accumulate and make a mass of accumulated unfolded proteins. Second, this mass disrupts the organelle compartment, and as a result, many chaperone proteins including the ER-resident protein PDI, are involved in this mass. Since these accumulated proteins expose the hydrophobic surface, it is easy for PDI to interact with these unfolded proteins by hydrophobic interaction. The co-localization of PDI and TDP-43 or SOD1 in NCIs could be linked to the formation of these inclusions.

One of the great puzzles in the study of ALS is why the motor system, and particular subsets of motor neurons, is selectively targeted for toxicity. Because of the accumulation of misfolding proteins, axon transport may be disturbed and make swollen neurites. As the motor neuron is the longest cell in the human nervous system, the motor system may be selectively disordered by the accumulation of misfolding proteins. We observed PDI-immunopositive swollen neurites in the patients with ALS. PDI may leave the injured ER and become to be aggregated in swollen axons due to disturbance of axon transport. In the ALS model mouse, axonal swelling is one of the early events and PDI is accumulated in the swollen axons in human ALS samples. However, further study is needed to find out weather it is a primary event or a late event.

In summary, we found co-localized inclusions of PDI with mutant SOD1 and TDP-43 in patients with ALS. The ER-specific chaperone protein PDI may leave the ER and then accumulate with SOD1 or TDP-43 in the cytosol. Furthermore, we found PDI-immunopositive swollen neurites in patients with SALS and FALS. As neurites are parts of the motor neuron, they are also degenerated. PDI may also accumulate in the swollen neurites due to the disturbance of axon transport. But the function of PDI

may be lost. These results suggest that the increase in the PDI activity may be a promising therapeutic strategy in ALS.

Acknowledgments

We thank Kumi Kodama and Nana Kawaguchi (Department of Pharmacoepidemiology, Kyoto University) for excellent technical assistance. This work was supported in part by a research grant from Eijinkai medical group in Japan.

Declaration of interest: The authors report no conflicts of interest. The authors alone are responsible for the content and writing of the paper.

References

(1) Wijesekera LC, Leigh PN. Amyotrophic lateral sclerosis. Orphanet J Rare Dis. 2009; 4: 3.

(2) Reaume AG, Elliott JL, Hoffman EK, Kowall NW, Ferrante RJ, Siwek DF, et al. Motor neurons in Cu/Zn superoxide dismutase-deficient mice develop normally but exhibit enhanced cell death after axonal injury. Nat Genet. 1996; 13: 43-7.

(3) Tu PH, Raju P, Robinson KA, Gurney ME, Trojanowski JQ, Lee VM. Transgenic mice carrying a human mutant superoxide dismutase transgene develop neuronal cytoskeletal pathology resembling human amyotrophic lateral sclerosis lesions. Proc Natl Acad Sci U S A. 1996; 93: 3155-60.

(4) Wegorzewska I, Bell S, Cairns NJ, Miller TM, Baloh RH. TDP-43 mutant transgenic mice develop features of ALS and frontotemporal lobar degeneration. Proc Natl Acad Sci U S A. 2009; 106: 18809-14.

(5) Nakamura T, Lipton SA. Cell death: protein misfolding and neurodegenerative diseases. Apoptosis. 2009; 14: 455-68.

(6) Noiva R, Lennarz WJ. Protein disulfide isomerase. A multifunctional protein resident in the lumen of the endoplasmic reticulum. J Biol Chem. 1992; 267: 3553-6.

(7) Tsai B, Rodighiero C, Lencer WI, Rapoport TA. Protein disulfide isomerase acts as a redox-dependent chaperone to unfold cholera toxin. Cell. 2001; 104: 937-48.

(8) Walker AK, Farg MA, Bye CR, McLean CA, Horne MK, Atkin JD. Protein disulphide isomerase protects against protein aggregation and is S-nitrosylated in amyotrophic lateral sclerosis. Brain. 2010; 133: 105-16.

(9) Honjo Y, Ito H, Horibe T, Takahashi R, Kawakami K. Protein disulfide isomerase-immunopositive inclusions in patients with Alzheimer disease. Brain Res. 2010; 1349: 90-6.

(10) Kawamoto Y, Akiguchi I, Shirakashi Y, Honjo Y, Tomimoto H, Takahashi R, et al Accumulation of Hsc70 and Hsp70 in glial cytoplasmic inclusions in patients with multiple system atrophy. Brain Res. 2007; 1136: 219-27.

(11) Kimura T, Hosoda Y, Kitamura Y, Nakamura H, Horibe T, Kikuchi M. Functional differences between human and yeast protein disulfide isomerase family proteins. Biochem Biophys Res Commun. 2004; 320: 359-65.

(12) Kimura T, Horibe T, Sakamoto C, Shitara Y, Fujiwara F, Komiya T, et al. Evidence for mitochondrial localization of P5, a member of the protein disulphide isomerase family. J Biochem. 2008; 144: 187-96.

(13) Kimura T, Nishida A, Ohara N, Yamagishi D, Horibe T, Kikuchi M. Functional

analysis of the CXXC motif using phage antibodies that cross-react with protein disulphide-isomerase family proteins. Biochem J. 2004; 382:169-76.

(14) Yamagishi S, Koyama Y, Katayama T, Taniguchi M, Hitomi J, Kato M, et al. An in vitro model for Lewy body-like hyaline inclusion/astrocytic hyaline inclusion: induction by ER stress with an ALS-linked SOD1 mutation. PLoS One. 2007; 2: e1030.

(15) Nishitoh H, Kadowaki H, Nagai A, Maruyama T, Yokota T, Fukutomi H, et al. ALS-linked mutant SOD1 induces ER stress- and ASK1-dependent motor neuron death by targeting Derlin-1. Genes Dev. 2008; 22:1451-64.

(16) Mori A, Yamashita S, Uchino K, Suga T, Ikeda T, Takamatsu K, et al. Derlin-1 overexpression ameliorates mutant SOD1-induced endoplasmic reticulum stress by reducing mutant SOD1 accumulation. Neurochem Int. 2011; 58:344-53.

(17) Urushitani M, Sik A, Sakurai T, Nukina N, Takahashi R, Julien JP. Chromogranin-mediated secretion of mutant superoxide dismutase proteins linked to amyotrophic lateral sclerosis. Nat Neurosci. 2006; 9:108-18.

(18) Atkin JD, Farg MA, Walker AK, McLean C, Tomas D, Horne MK. Endoplasmic reticulum stress and induction of the unfolded protein response in human sporadic amyotrophic lateral sclerosis Neurobiol Dis. 2008; 30: 400-7.

(19) Williamson TL, Cleveland DW. Slowing of axonal transport is a very early event in the toxicity of ALS-linked SOD1 mutants to motor neurons. Nat Neurosci. 1999; 2: 50-6.

Figure Legends

Fig. 1

(A) Neurons (arrows) in normal cervical spinal cord were immunopositive for PDI. (B) Oligodendrocytes (arrowhead) and neurites (arrows) in normal cervical spinal cord were also immunostained by the anti-PDI antibody. Scale bars: 20 μm.

Fig. 2

Anti-PDI-antibody-immunopositive NCI (arrow) from a patient with (A) SALS (cervical spinal cord) and (B) FALS (cervical spinal cord). Scale bars: 10 μm.

Fig. 3

(A) Anti-PDI-antibody-immunopositive swollen neurites (arrows) and degenerated neurons (arrowheads) from a patient with FALS (cervical spinal cord). (B) Anti-PDI-antibody-immunoreactive swollen neurites (arrow) from a patient with SALS (cervical spinal cord). Scale bars: 20 μm.

Fig. 4

Double immunostaining of NCIs from a patient with SALS (cervical spinal cord). TDP-43 and PDI are co-localized in NCIs (arrow). Green: anti-PDI antibody immunostaining (A). Red: anti-TDP-43 antibody immunostaining (B). Yellow: merged

immunostaining (C). *Differential interference contrast* (DIC): (D). Scale bar: 20 μm.

Fig. 5

Double immunostaining of NCI from a patient with FALS (cervical spinal cord). SOD1 and PDI are co-localized in NCI (arrow). Green: anti-PDI antibody immunostaining (A). Red: anti-SOD1 antibody immunostaining (B). Yellow: merged immunostaning (C). *Differential interference contrast* (DIC): (D). Scale bar: 20 μm.

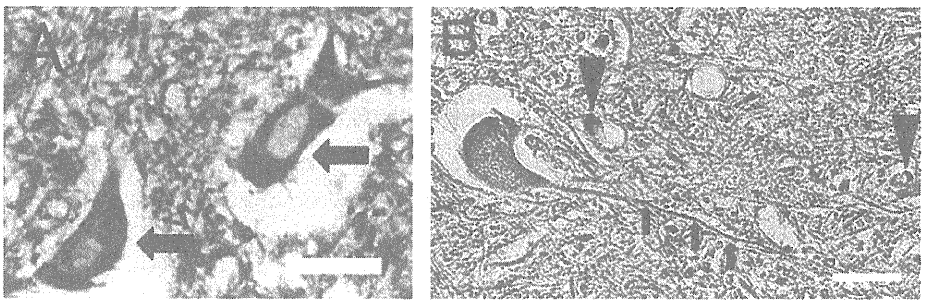

Figure 1
(A) Neurons (arrows) in normal cervical spinal cord were immunopositive for PDI. (B) Oligodendrocytes (arrowhead) and neurite (arrows) in normal cervical spinal cord were also immunostained by the anti-PDI antibody. Scale bars: 20 μm.

34x10mm (600 x 600 DPI)

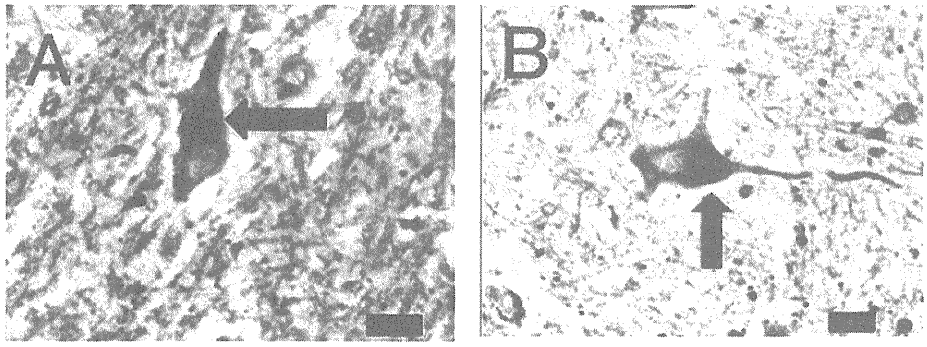

Figure2
Anti-PDI-antibody-immunopositive NCI (arrow) from a patient with (A) SALS (cervical spinal cord) and (B) Anti-PDI-antibody-immunoreactive NCI (arrow) from a patient with FALS (cervical spinal cord). Scale bars: 10 μm.
34x12mm (600 x 600 DPI)

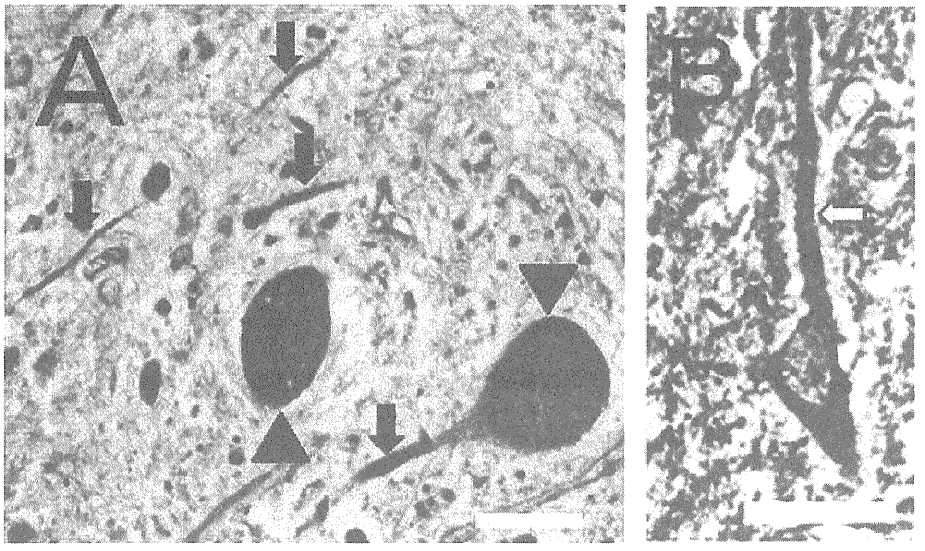

Figure 3
(A) Anti-PDI-antibody-immunopositive swollen neurites (arrows) and degenerated neurons (arrow heads) from a patient with FALS (cervical spinal cord). (B) Anti-PDI-antibody-immunoreactive swollen neurite (arrow) from a patient with SALS (cervical spinal cord). Scale bars: (A, B) 20 µm.

22x13mm (600 x 600 DPI)

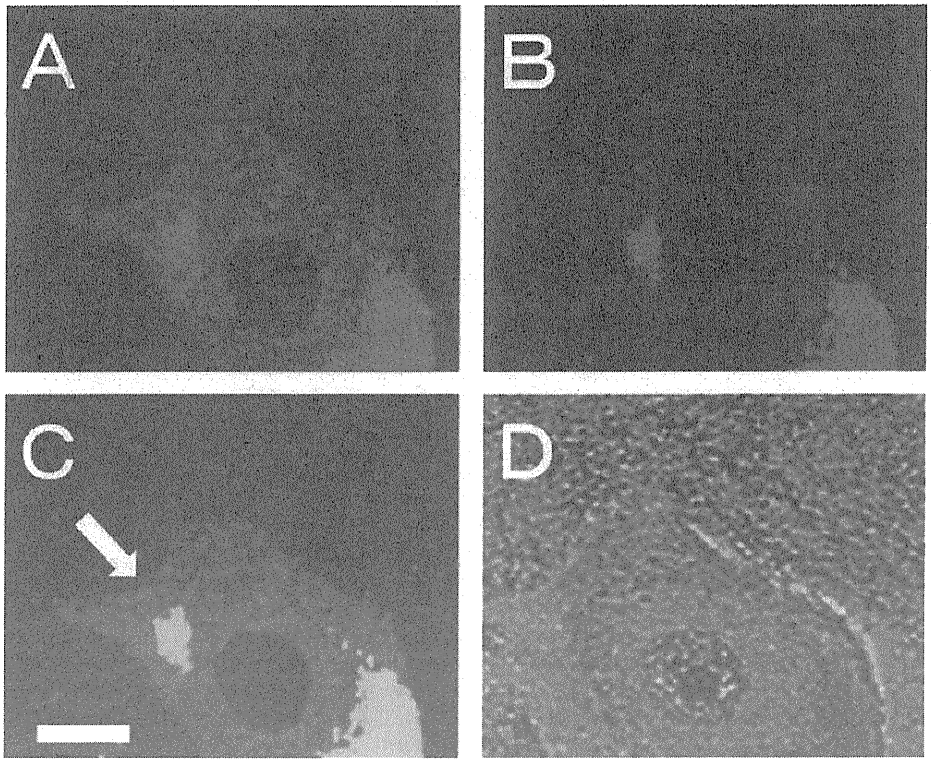

Figure 4
Double immunostaining of NCIs from a patient with SALS (cervical spinal cord). TDP-43 and PDI are co-localized in NCIs (arrow). Green: anti-PDI antibody immunostaining (A). Red: anti-TDP-43 antibody immunostaining (B). Yellow: merged immunostaining (C). Differential interference contrast (DIC): (D). Scale bar: 20 μm.
54x44mm (600 x 600 DPI)

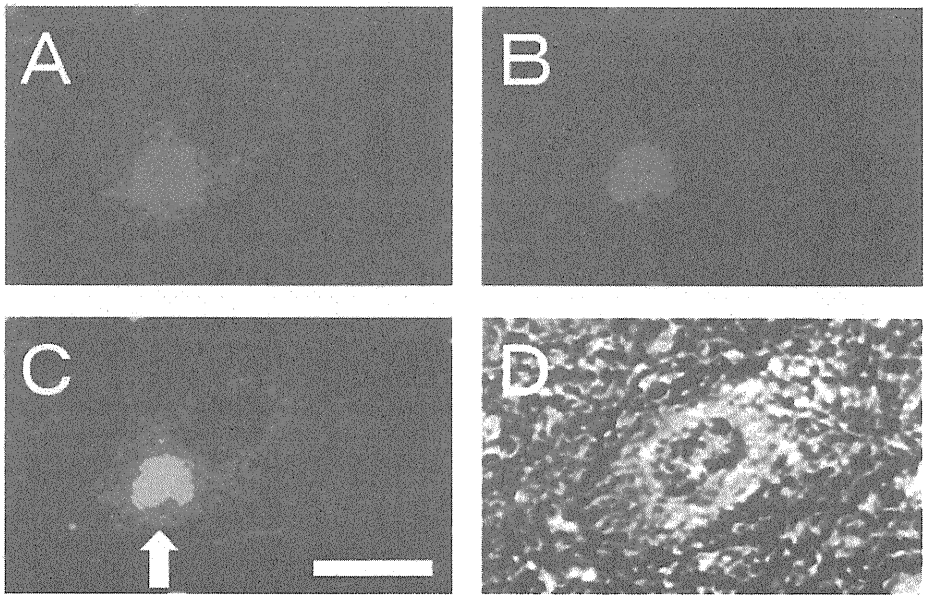

Figure 5
Double immunostaining of NCI from a patient with FALS (cervical spinal cord). SOD1 and PDI are co-localized in NCI (arrow). Green: anti-PDI antibody immunostaining (A). Red: anti-SOD1 antibody immunostaining (B). Yellow: merged immunostaning (C). Differential interference contrast (DIC): (D). Scale bar: 20 μm.
59x37mm (600 x 600 DPI)

Acta Neuropathol (2011) 122:223–229
DOI 10.1007/s00401-011-0842-y

ORIGINAL PAPER

Clinicopathologic study on an ALS family with a heterozygous E478G *optineurin* mutation

Hidefumi Ito · Masataka Nakamura · Osamu Komure · Takashi Ayaki · Reika Wate · Hirofumi Maruyama · Yoshimi Nakamura · Kengo Fujita · Satoshi Kaneko · Yoko Okamoto · Masafumi Ihara · Tetsuro Konishi · Kazumasa Ogasawara · Asao Hirano · Hirofumi Kusaka · Ryuji Kaji · Ryosuke Takahashi · Hideshi Kawakami

Received: 10 April 2011 / Accepted: 20 May 2011 / Published online: 5 June 2011

Abstract We investigated a family manifesting amyotrophic lateral sclerosis (ALS) with a heterozygous E478G mutation in the *optineurin* (*OPTN*) gene. Clinically, slow deterioration of motor function, mood and personality changes, temporal lobe atrophy on neuroimaging, and bizarre finger deformity were noted. Neuropathologically, TAR DNA-binding protein 43 (TDP-43)-positive neuronal intracytoplasmic inclusions were observed in the spinal and medullary motor neurons. In these cells, the immunoreactivity of nuclear TDP-43 was reduced. Consecutive sections revealed that the inclusions were also reactive with anti-ubiquitin and anti-p62 antibodies, but noticeably negative for OPTN. In addition, TDP-43/p62-positive glial cytoplasmic inclusions (GCIs) were scattered throughout the spinal cord and the medullary motor nuclei. Furthermore, Golgi fragmentation was identified in 70% of the anterior horn cells (AHCs). The presence of AHCs with preserved nuclear TDP-43 and a fragmented Golgi apparatus, which are unrecognizable in sporadic ALS, indicates that patients with the E4787G *OPTN* mutation would manifest Golgi fragmentation before loss of nuclear TDP-43. In the neocortex, GCIs were sparsely scattered among the primary motor and temporal cortices, but no neuronal TDP-43-positive inclusions were detected. In the amygdala and the ambient gyrus, argyrophilic grains and ballooned neurons were seen. The thorough neuropathologic investigations performed in this work demonstrated that OPTN-positive inclusion bodies, if any, were not prominent. We postulate that optineurinopathy is closely linked with TDP-proteinopathy and speculate that this heterozygous E478G mutation would cause ALS by acting through a dominant-negative mechanism.

Keywords Amyotrophic lateral sclerosis · Optineurin · TDP-43 · Golgi fragmentation

Electronic supplementary material The online version of this article (doi:10.1007/s00401-011-0842-y) contains supplementary material, which is available to authorized users.

H. Ito (✉) · T. Ayaki · Y. Okamoto · M. Ihara · R. Takahashi
Department of Neurology, Kyoto University Graduate School of Medicine, 54 Kawahara-cho, Shogoin, Sakyo-ku, Kyoto 606-8507, Japan
e-mail: itohid@kuhp.kyoto-u.ac.jp

M. Nakamura · R. Wate · Y. Nakamura · K. Fujita · S. Kaneko · H. Kusaka
Department of Neurology, Kansai Medical University, Osaka 570-8507, Japan

O. Komure
Shin-ai Hospital, Osaka 569-1123, Japan

H. Maruyama · H. Kawakami
Department of Epidemiology, Research Institute for Radiation Biology and Medicine, Hiroshima University, Hiroshima 734-8553, Japan

T. Konishi
National Hospital Organization Utano Hospital, Kyoto 616-8255, Japan

K. Ogasawara
Department of Pathology, School of Medicine, Shiga University of Medical Science, Shiga 520-2192, Japan

A. Hirano
Division of Neuropathology, Department of Pathology, Montefiore Medical Center, New York, NY 10467, USA

R. Kaji
Department of Clinical Neuroscience, University of Tokushima Graduate School, Tokushima 770-8503, Japan

Introduction

We recently reported that mutations in the gene encoding optineurin (*OPTN*) cause amyotrophic lateral sclerosis (ALS) [15]. *OPTN* had previously been identified as a causative gene of primary open-angle glaucoma (POAG) [18]. However, the sites of mutation in the *OPTN* gene found in ALS patients were distinct from those in cases with POAG. In addition, we demonstrated that OPTN is co-localized with TAR DNA-binding protein of 43 kDa (TDP-43) or Cu/Zn superoxide dismutase (SOD1) in the pathognomonic inclusion bodies of sporadic ALS (SALS) or familial ALS associated with *SOD1* mutation (SOD1-FALS), respectively [15]. The presence of OPTN immunoreactivity in TDP-43-positive inclusions of SALS patients was subsequently confirmed by other investigators [9, 17]. In addition, we recently demonstrated that OPTN is also co-localized with *fused* in *sarcoma* (FUS) within basophilic inclusions of ALS with the *FUS* mutation and in basophilic inclusion body disease [10]. Our findings thus indicate that OPTN associates with each of three major ALS-related proteins, i.e., TDP-43, SOD1, and FUS, suggesting that the underlying pathomechanism in ALS might be attributable to dysfunctional OPTN.

We identified eight ALS cases associated with three distinct types of *OPTN* mutation (OPTN-ALS) [15]: two siblings with a homozygous deletion of exon 5, two cases with a homozygous Q398X nonsense mutation, and four patients with a heterozygous E478G missense mutation within its ubiquitin-binding domain. Detailed clinicopathological features of patients with each mutation remain unknown. Moreover, whereas the pathomechanism causing the disease by the homozygous mutations is speculated to be a loss of function resulting from nonsense-mediated mRNA decay of the transcript, that of the heterozygous E478G mutation remains uncertain.

Here, we provide further clinicopathologic information about Family 4 [15] with the E478G mutation. Although their clinical features and our neuropathologic findings have previously been reported in brief [15], we obtained some new and novel information by examining the living patient and interviewing her daughters, and by investigating the autopsied material thoroughly.

Subjects and methods

Clinical features

Three siblings were affected in this family (Fig. 1a). Their mother died at age 32 from heart disease. Their father then married the mother's younger sister and had four more children (denoted by the diamond symbol). The father was over 80 years old at death, and all of his other four children are now over 60 years of age with no signs of ALS.

The demographic and clinical features of the three OPTN-ALS patients are summarized in Table 1.

Patient III-1 had noted right-hand weakness at age 58. Muscle weakness of all four limbs, dysarthria, and dysphagia followed. Her nieces noticed that she had become irritable and touchy. She was diagnosed as having ALS and died of pneumonia after artificial ventilation for several months at age 63.

Patient III-2 suffered from right-hand weakness at age 56. Flexion deformity of her fingers gradually developed four years later. Examinations at age 61 disclosed dysarthria, atrophy, fasciculation in the tongue, and exaggerated deep tendon reflexes and bilateral extensor plantar responses in all four extremities. She was depressed but not demented. A cranial MRI demonstrated mild atrophy of the medial temporal region (Fig. 1b). She died of CO_2 narcosis without respiratory support at age 66.

Patient III-3 suffered from right-hand weakness at age 64. Leg weakness, dysarthria, and dysphagia followed slowly afterward. She could communicate well with others until age 75, when she became taciturn and depressive. A cranial CT scan at age 76 showed pronounced temporal lobe atrophy (Fig. 1c). Examinations at age 78 revealed generalized atrophy and fasciculation of skeletal muscles, reduced deep tendon reflexes, and bilateral extensor plantar responses. Atrophy of the tongue was mild. Conspicuously, her fingers were bizarrely deformed, resulting in difficulty in passive movement of any finger joints (Fig. 1d). We observed 4-Hz rhythmic tremor of the fingers of her left hand. She was awake, and eye contact was preserved, but appeared expressionless and mute. She is alive after 14 years from the onset without respiratory support.

No patients developed decubitus, ophthalmoplegia, glaucoma, or cardiac or muscular abnormalities. Blood tests, including those on alkaline phosphatase and creatine phosphokinase, were normal. Chest and spine X-rays did not show any evidence of Paget's disease.

We had previously identified a heterozygous missense mutation (c.1743A>G, E478G, exon14) in the *OPTN* gene of Patients III-2 and III-3 [15]. Genetic analysis and cognitive testing were not performed on the other family members because of the lack of informed consent.

Neuropathological examinations

Formalin-fixed, paraffin-embedded 6-μm-thick sections were deparaffinized and stained with hematoxylin and eosin (H&E) or subjected to Gallyas–Braak silver impregnation. For immunohistochemistry, after antigen retrieval by heat/autoclaving (10 min at 121°C in 10 mM sodium citrate buffer, pH 6.0), the sections were incubated with a given

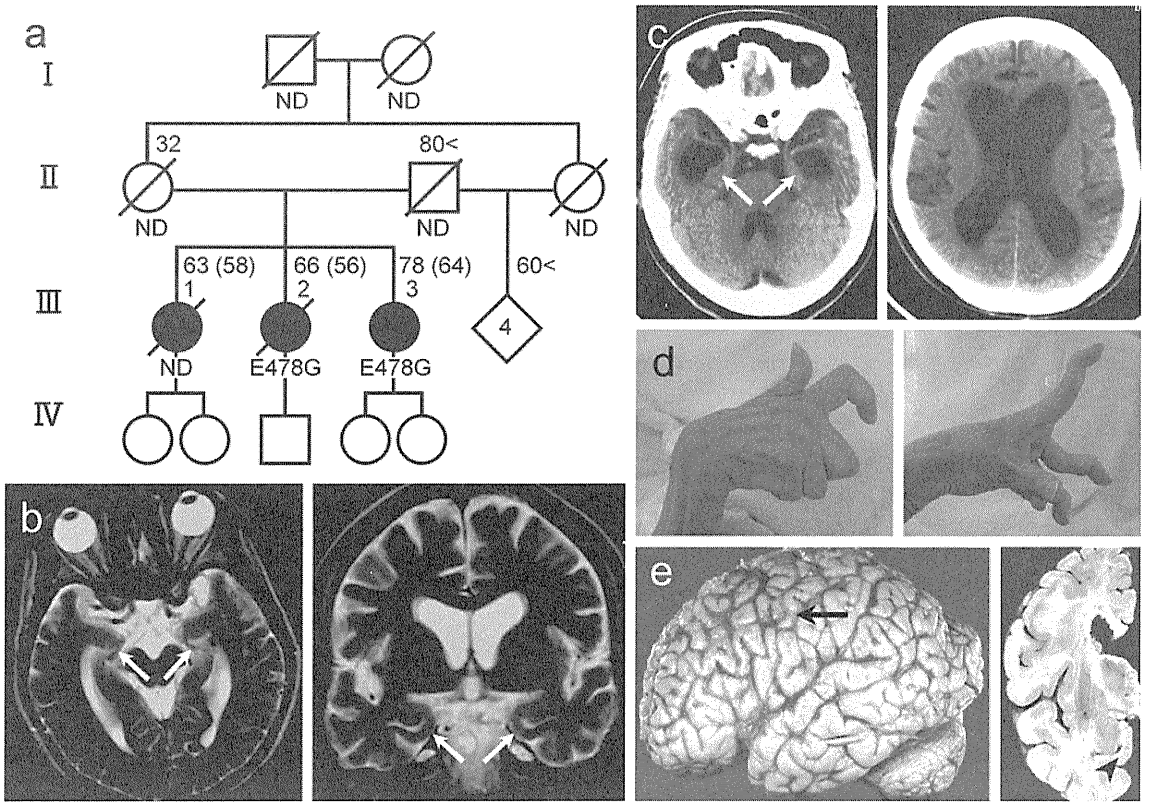

Fig. 1 Clinical and neuropathologic findings of the familial amyotrophic lateral sclerosis (FALS) patients with an *optineurin* (*OPTN*) mutation. The three patients in the family pedigree are indicated by the *solid circles* (**a**). A heterozygous E478G mutation in the *OPTN* gene was detected in Patients III-2 and III-3. *ND* not determined. Age at death or current age and age at disease onset are indicated *n (m)*. Deceased individuals are indicated by the *oblique line*. A cranial MRI of Patient III-2 at age 65 (**b**) reveals mild atrophy of the ambient gyri (*arrows*). A cranial CT scan of Patient III-3 at age 76 (**c**) reveals conspicuous atrophy of the medial temporal lobes (*arrows*) and mild atrophy of the frontal lobe. Gradually progressive bizarre deformity of the hands of Patient III-3 is striking (**d**). Photographs of the brain from Patient III-2 (**e**) reveal slight atrophy of the motor cortex (*arrow*) and of the ambient gyrus (*arrowhead*)

Table 1 Demographic and clinical features of patients with a heterozygous E478G *OPTN* mutation

Patient	III-1	III-2	III-3
Age at onset (years)	58	56	64
Gender	Female	Female	Female
Symptom at onset	Right-hand weakness	Right-hand weakness	Right-hand weakness
Upper motor neuron signs	Unknown	+	+
Lower motor neuron signs	+	+	+
Cognitive symptoms	Personality change	Depression	Depression
Other clinical features	–	Finger deformity	Finger deformity, Parkinsonian tremor
Neuroimaging	Unknown	Mild temporal lobe atrophy	Marked temporal lobe atrophy
Disease duration (years)	5	10	>14
Artificial ventilation	For several months	–	–
Cause of death	Pneumonia	CO_2 narcosis	Alive
Genetic analysis	Unavailable	E478G in *OPTN* gene	E478G in *OPTN* gene

primary antibody (listed in Online Resource 1) overnight at 4°C. Bound antibodies were detected with the appropriate Vectastain Elite ABC kit (Vector Laboratories, Burlingame, CA, USA), with 3,3′-diaminobenzidine tetrahydrochloride used as the chromogen. All sections were counterstained with hematoxylin after immunohistochemistry. Some sections were stained with H&E, photographed, decolorized with 70% ethanol, and then immunostained for OPTN. The tissues from three age-matched neurologically normal subjects served as controls.

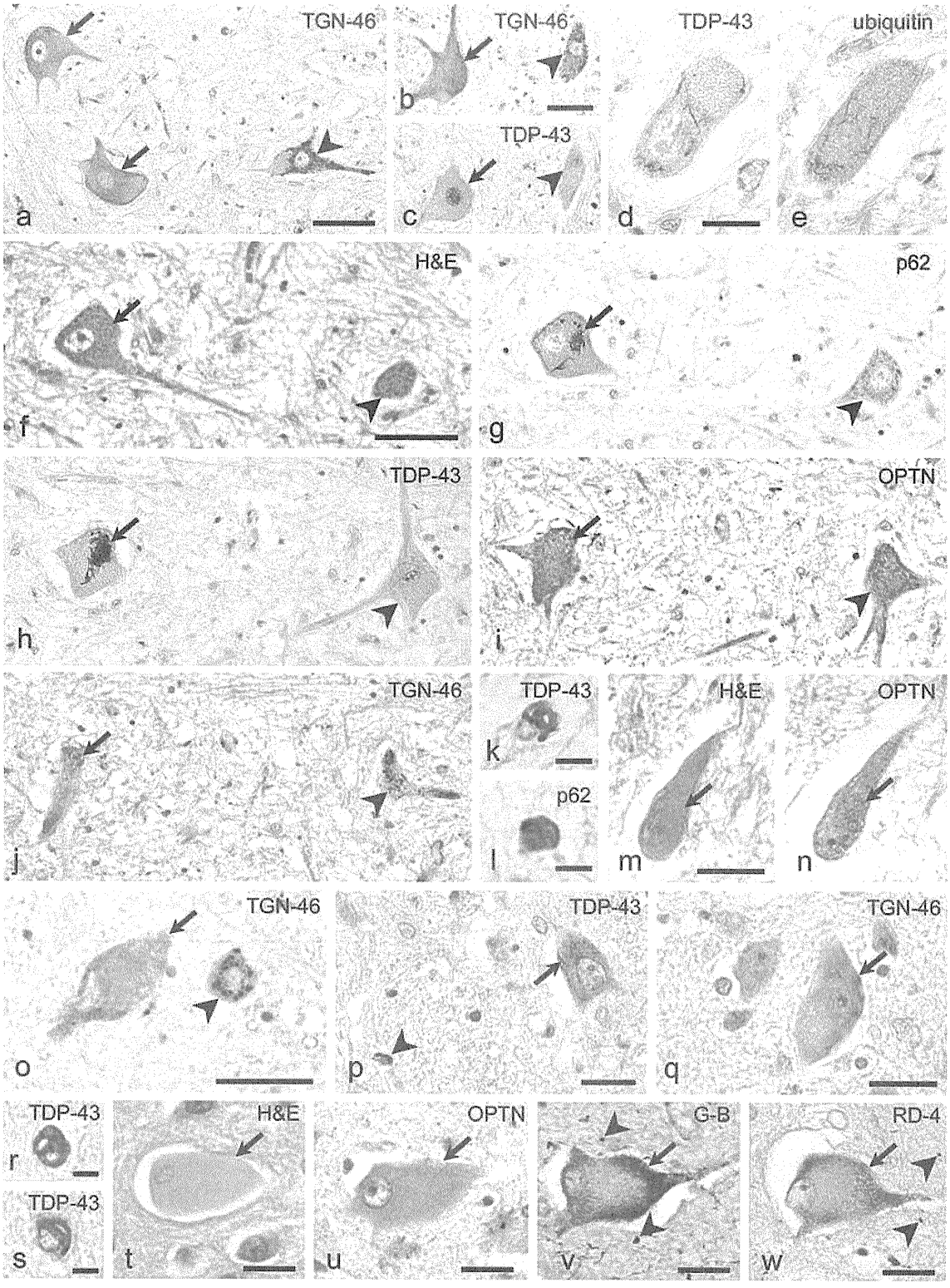

We assessed staining specificity by replacing the primary antibodies with an appropriate amount of non-immune rabbit serum or phosphate-buffered saline solution containing 3% bovine serum albumin. No deposits of reaction products were seen in the sections thus treated (data not shown).

Procedures involving use of human material were performed in accordance with ethical guidelines set by Shiga University of Medical Science and the Helsinki Declaration of 1983. No frozen tissue was available.

◀ **Fig. 2** Representative photomicrographs of the lumbar anterior horn (**a**–**n**), the facial nucleus (**o**, **p**), and the cerebral cortices (**q**–**w**) from Patient III-2. Immunostaining with anti-trans-Golgi-network 46 (*TGN-46*) antibody demonstrates evident fragmentation of the Golgi apparatus (GA) in some of the anterior horn cells (AHCs, *arrows*), in comparison with the preserved GA (*arrowhead*) in others (**a**). Consecutive sections stained with anti-TGN-46 (**b**) and anti-TDP-43 (**c**) antibodies indicate a neuron with normal nuclear TDP-43 immunoreactivity and obviously fragmented GA (*arrow*). The other neuron in these sections has a normal GA with preserved TDP-43 nuclear staining (*arrowhead*). A noticeable skein-like cytoplasmic inclusion immunoreactive for TDP-43 (**d**) and ubiquitin (**e**) is identifiable in consecutive sections. The physiological nuclear TDP-43 immunoreactivity is absent (**d**). Five consecutive sections stained with H&E (**f**) and immunostained for p62 (**g**), TDP-43 (**h**), optineurin (**i**), and GA (**j**) in this order reveal that a TDP-43-positive skein-like inclusion (**h**, *arrow*) is also reactive with anti-p62 antibody (**g**, *arrow*), which inclusion is indiscernible on the H&E-stained section (**f**, *arrow*). Note that the inclusion is devoid of optineurin (OPTN-I)-labeling (**i**, *arrow*). The GA is fragmented in this neuron (**j**, *arrow*) compared with the spared AHC with preserved TDP-43 nuclear staining (**f**–**j**, *arrowheads*). Glial cytoplasmic inclusions (GCIs) immunoreactive with anti-TDP-43 (**k**) and anti-p62 (**l**) antibodies are scattered throughout the spinal cord. The eosinophilic cytoplasmic hyaline region of this ÂHC (**m**) was decolorized and re-stained with the OPTN-C antibody (**n**), resulting in positive staining; however, prominent OPTN-positive inclusion bodies were not evident. GA fragmentation is apparent in this motor neuron of the facial nucleus immunostained with TGN-46 antibody (**o**, *arrow*), whereas another neuron has a preserved GA (*arrowhead*). By staining with anti-TDP-43 antibody, a skein-like inclusion (**p**, *arrow*) and a GCI (*arrowhead*) are clearly identifiable in the facial nucleus. A Betz cell within the primary motor cortex (**q**) shows reduced immunoreactivity with TGN-46 antibody (*arrow*). Only sparsely scattered TDP-43-positive GCIs are detectable in the frontal (**r**) and the temporal (**s**) cortices. Ballooned neurons in the ambient gyrus (**t**–**w**, *arrows*) are immunopositive in their entire cytoplasm for OPTN (**u**), stained at their periphery by Gallyas–Braak (*G–B*) silver staining (**v**, *arrow*), and are reactive with anti-4-repeat tau (*RD-4*) antibody (**w**, *arrow*). Argyrophilic grains (**v**, *arrowheads*), immuno-positive for 4-repeat tau (**w**, *arrowheads*), are also observed. *Scale bars* 50 μm (**a**, **b**, **f**, **o**), 20 μm (**d**, **m**, **p**, **q**, **t**–**w**), and 10 μm (**k**, **l**, **r**, **s**)

Results

The brain of Patient III-2 weighed 1,250 g. Macroscopically, the primary motor and medial temporal cortices appeared slightly atrophic (Fig. 1e).

Throughout the spinal cord, the anterior horns and the corticospinal tracts had degenerated. Additional immunohistochemical investigation revealed characteristic fragmentation of the Golgi apparatus (GA) in the anterior horn cells (AHCs; Fig. 2a). Quantitative analysis using a method described elsewhere [8] revealed that 72.8% (75/103) of the AHCs from eight distinct spinal cord segments had fragmented GAs. Analysis of consecutive sections immunostained for GA and TDP-43 revealed GA fragmentation not only in all the AHCs with reduced nuclear TDP-43 immunoreactivity but also in a substantial number of those with preserved nuclear TDP-43 (Fig. 2b, c). In contrast, a normal staining pattern for GAs was observed for non-motor neurons.

More importantly, we identified TDP-43/ubiquitin-positive skein-like inclusions in AHCs (Fig. 2d, e). The nucleus of these inclusion-bearing neurons was invariably immunonegative for TDP-43. Consecutive sections revealed that the TDP-43-positive inclusions were also reactive with anti-p62 antibody; they were difficult to recognize on H&E-stained sections and noticeably negative for OPTN on use of either the OPTN-C or OTPN-I antibodies (Fig. 2f–i). This finding was confirmed by double immunofluorescence investigation (Online Resource 2). The GA in AHCs with such inclusions was fragmented (Fig. 2j). We identified inclusions in 12.5% (19/152) of AHCs on 20 cervical and lumbar cord sections immunostained for TDP-43. In addition, TDP-43/p62-positive glial cytoplasmic inclusions (GCIs) were scattered throughout the spinal cord (Fig. 2k, l).

Careful examination of 265 AHCs on 30 H&E-stained sections revealed no Bunina bodies or round hyaline inclusions in these cells. Cystatin C immunohistochemistry failed to detect Bunina bodies in 182 AHCs examined. Eosinophilic intracytoplasmic regions were noted in several AHCs, which showed immunoreactivity when decolorized and then re-stained with each of the anti-OPTN antibodies (Fig. 2m, n). Occasionally, these eosinophilic retentions appeared to have formed inclusion-like structures; however, OPTN-positive prominent inclusion bodies delineated by a distinct margin were completely unrecognizable.

In the hypoglossal and facial nuclei, motoneurons were depleted in number, the GA was fragmented, and TDP-43-positive inclusions were identified (Fig. 2o, p). Betz cells were mildly depleted in number, and the remaining cells had reduced immunoreactivity for GA (Fig. 2q). TDP-43-immunoreactive GCIs were sparsely scattered among the medullary motor nuclei (Fig. 2p), primary motor and temporal cortices (Fig. 2r, s), putamen, and thalamus, but no neuronal intracytoplasmic inclusions were found other than in the spinal and medullary motor neurons. No intranuclear inclusions were identifiable throughout the central nervous system.

In the amygdala and the ambient gyrus, numerous argyrophilic, 4-repeat tau-positive grains, and several ballooned neurons were seen (Fig. 2t–w). The cytoplasm of these neurons was eosinophilic, and diffusely immunopositive for OPTN and phosphorylated neurofilaments; the cells were stained at their periphery by Gallyas–Braak silver impregnation and with anti-4-repeat tau antibody. There was faint, if any, immunoreactivity indicating ubiquitin, and the cells were negative for p62, α-synuclein, 3-repeat tau, TDP-43, FUS, SOD1, and ApoE. This III-2 case corresponded to argyrophilic grain disease (AGD), stage II [5, 20].

By amyloid β and AT8-immunohistochemistry this case was graded as amyloid stage A and NF stage II,